Berry phase in a weakly anharmonic qubit coupled to a microwave resonator (Semester paper)

Marek Pechal

September 7, 2010

Contents

1 Introduction

An important result of quantum mechanics – the adiabatic theorem [1] – states that a system with a Hamiltonian slowly varying in time[1] follows the instantaneous eigenstate of this Hamiltonian (i.e. if the system is in an eigenstate of the initial Hamiltonian, it will also be in an eigenstate of the Hamiltonian at any later time). However, the theorem does not specify the phase of the eigenstate. As noted by Berry [2], during a cyclic adiabatic evolution of the Hamiltonian, an eigenstate accumulates a non-trivial geometric phase

[1] This is of course a rather vague statement. As a rule of thumb, the evolution of the Hamiltonian can be considered adiabatic if the rate of change of its eigenvectors is much slower than the differences between its eigenenergies.

in addition to the dynamical phase given by the time integral of its eigenenergy. This geometric phase only depends on the trajectory followed by the Hamiltonian in the space of hermitian operators and not on the total duration of the evolution. Moreover, it is expected to be relatively stable under perturbations of the Hamiltonian [3].

These properties make geometric phase a promising resource for quantum information processing. Quantum gates based on adiabatic evolution could provide better fidelities than simple dynamical gates. Obviously, as a first step towards building such geometric quantum gate it is necessary to observe geometric phase in a quantum bit and study its properties until all relevant phenomena are well-understood (e.g. the influence of higher qubit levels, the microwave cavity or other elements of the qubit environment such as free electromagnetic modes whose coupling to the qubit causes its relaxation and dephasing etc.).

An experiment aimed at measuring the geometric phase in a transmon superconducting qubit has been recently performed by Simon Berger at the Quantum Device Lab of the ETH Zurich. The results have shown an unexpected deviation from theoretical predictions.

The aim of this semester paper is to explain the observed deviation theoretically.

2 Description of the experiment

The qubit used in this experiment is a transmon superconducting qubit [4] embedded in a transmission line resonator. It can be approximated as a weakly anharmonic oscillator operated in a regime where all transitions except between the two lowest levels can be neglected. This approximation results in the usual model of a cavity QED system [5] described by the well known Jaynes-Cummings Hamiltonian.

The qubit and the resonator are far detuned from each other (i.e. the detuning $\omega_r - \omega_q$ is much larger than the coupling g between the resonator and the qubit). In this so-called dispersive limit, the Hamiltonian can be transformed into a form where these two subsystems are effectively decoupled except for a Stark shift of their energy levels. Also a drive signal at the input of the resonator translates into a direct drive of the qubit.

The qubit can then be considered as a simple two-level system. In a frame corotating at the external drive frequency around the z-axis, such system can be thought of as a spin $1/2$ in a magnetic field whose z-component is the detuning between the qubit and drive frequency and whose x and y-components are the two quadratures of the drive signal.

In this experiment, the amplitude of the drive was adiabatically increased at constant detuning and then kept constant while the phase shift was increased from 0 to 2π, thus making the vector of the effective magnetic field trace a conical path with a given opening angle. Finally, the drive amplitude was decreased back to zero. As a result of this sequence, the ground and excited state of the qubit acquire phases consisting of a dynamical and geometric contribution. The dynamical phase was eliminated by means of a spin echo technique – the adiabatic sequence was performed twice, each time with a different orientation of the path. The change of direction of the path leaves the dynamical phase invariant while changing the sign of the geometric phase – therefore the spin echo sequence results in the ground and excited state being phase-shifted with respect to each other by twice the difference between their geometric phases.

If the system is initially prepared in a superposition state of the ground and excited state then the phase difference resulting from this procedure can be determined by tomography of the final state.

Should the geometric phase be simply equal to half the solid angle $\mathcal{A}$ subtended by the path as derived by Berry [2] for a two-level system, then the phase ϕ measured by the spin echo experiment would be given by $\phi = 2\mathcal{A}$. However, the real experimental results clearly exhibit a deviation from this linear dependence, as can be seen in Figure 1 in a plot of the measured phase as a function of the solid angle for detuning equal to -50 MHz. Here the solid line is the theoretical dependence $\phi = 2\mathcal{A}$ while the dots are the experimental results.

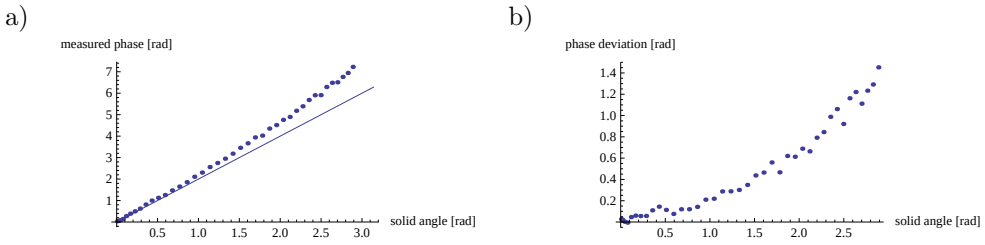

Figure 1: The phase measured for detuning -50 MHz as a function of the solid angle compared with the theoretical prediction for an ideal 2-level system (a) and the difference between them (b).

In the following we will study two effects which could possibly lead to a deviation of the geometric phase from Berry's two-level result and compare the obtained theoretical predictions with experimental data.

We should note that the geometric phase has now been measured many times for different parameters of the system during several measurement sessions and there are many data sets available to compare our theories with. However, the data are not always perfectly consistent which suggests that there are still some aspects to the measurements yet to be understood.

Since this text is not intended to serve as a comprehensive overview of the obtained experimental results, we only present comparisons of our theoretical predictions with a small subset of the measurements. Our choice of this subset is to some degree arbitrary. Generally, we attempted to choose data sets not deviating significantly from what we saw as a "typical" result and containing as little noise as possible.

A much more detailed description of the experiment can be found in Simon Berger's master thesis.

3 Corrections due to higher qubit levels

The first effect that we consider as a possible cause of the observed deviation is the presence of higher qubit levels. This explanation seems reasonable because any effect the higher levels might have on the geometric phase could be especially pronounced in a transmon qubit due to its low anharmonicity compared to other superconducting qubit designs. Moreover, an experiment very similar to the one described here has been used

to measure the geometric phase in a Cooper pair box [6] with results significantly closer to the theoretically predicted linear dependence on solid angle. One of the differences between the two experiments which might explain the different results is, among others, the different relative anharmonicity of the qubits. A closer look at the differences and similarities of the two experiments could provide a helpful insight into why the deviation of the experimental results from theoretical predictions is so much larger for a transmon qubit than for a Cooper pair box.

3.1 Geometric phase in a multilevel system following a conical path

Let us consider a general Hamiltonian of the tridiagonal form

$$\hat{H}(\varphi) = \hat{D} + (\hat{\Sigma}^{+}\mathrm{e}^{-\mathrm{i}\varphi} + \mathrm{h.c.}),$$

where $\hat{D}$ is diagonal in some basis consisting of vectors $|0\rangle, |1\rangle, \ldots$ while $\langle i|\hat{\Sigma}^{+}|j\rangle$ is only non-zero if $i = j + 1$. The Hamiltonian of a multilevel qubit belongs into this class of operators. In a frame corotating with the drive frequency ω_d it is equal to

$$\frac{1}{\hbar}\hat{H}(\varphi) = \sum_n (n\delta + \alpha_n)|n\rangle\langle n| + \frac{1}{2}\sum_n (\Omega g_{n,n+1}\mathrm{e}^{-\mathrm{i}\varphi}|n+1\rangle\langle n| + \mathrm{h.c.}). \tag{1}$$

Here the anharmonicity α_n is defined as $\omega_n = n\omega_q + \alpha_n$ with $\alpha_0 = \alpha_1 = 0$ and the detuning δ as $\omega_q - \omega_d$. The constants $g_{n,n+1}$ express coupling strengths between levels n and $n+1$ relative to the $0 \leftrightarrow 1$ coupling (i.e. $g_{01} = 1$). For a weakly anharmonic qubit [4] they can be approximated as $g_{n,n+1} = \sqrt{n+1}$.

The drive amplitude Ω and the phase φ are related to the two drive quadratures by $\Omega_x = \Omega\cos\varphi$ and $\Omega_y = \Omega\sin\varphi$. Therefore – in terms of our analogy with the spin 1/2 in a magnetic field – if the phase φ runs from 0 to 2π then the effective magnetic field traces a conical path with an opening angle θ (see Figure 2) given by $\cos\theta = \delta/\sqrt{\delta^2 + \Omega^2}$ enclosing a solid angle $\mathcal{A} = 2\pi(1 - \cos\theta)$.

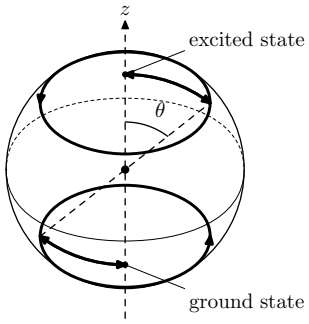

Figure 2: Trajectories followed by the ground and the excited state of the qubit on the Bloch sphere during the adiabatic sequence.

To calculate corrections due to the higher levels we will make use of the fact that the dependence of the Hamiltonian on φ can be expressed in terms of a simple unitary transformation. Let us define an operator

$$\hat{N} = \sum_n n|n\rangle\langle n|.$$

The Hamiltonian can then be expressed as

$$\hat{H}(\varphi) = \mathrm{e}^{-\mathrm{i}\varphi\hat{N}}\hat{H}(0)\mathrm{e}^{\mathrm{i}\varphi\hat{N}}.$$

Therefore if $|\Phi\rangle$ is an eigenvector of $\hat{H}(0)$ then $|\Phi(\varphi)\rangle = \mathrm{e}^{-\mathrm{i}\varphi\hat{N}}|\Phi\rangle$ is the corresponding eigenvector of $\hat{H}(\varphi)$.

Hence if the parameter φ of the Hamiltonian is adiabatically varied from 0 to 2π, the geometric phase accumulated by the eigenvector $|\Phi\rangle$ is given by [2]

$$\gamma_\Phi = \mathrm{i}\int_0^{2\pi} \langle\Phi(\varphi)|\frac{\mathrm{d}}{\mathrm{d}\varphi}|\Phi(\varphi)\rangle\,\mathrm{d}\varphi = 2\pi\langle\Phi|\hat{N}|\Phi\rangle. \tag{2}$$

We can check that this relation indeed gives the correct result for a conical path in an ideal two-level system. In this case the operator $\hat{N}$ is equal to $(\mathbb{1} + \hat{\sigma}_z)/2$ and equation (2) simplifies to

$$\gamma_\Phi = 2\pi\langle\Phi|\frac{\mathbb{1} + \hat{\sigma}_z}{2}|\Phi\rangle = \pi(1 \pm \cos\theta), \tag{3}$$

where the sign $\pm$ corresponds to the positive and negative eigenvalue of $\hat{H}(0)$ respectively. This expression differs from Berry's result only by an unobservable multiple of 2π.

3.2 Perturbative calculation of the higher levels correction

The following section describes a calculation of the lowest order perturbative correction to the geometric phase caused by the presence of higer qubit levels. It proceeds as a rather straightforward application of the non-degenerate perturbation theory and is included here for completeness.

Since we want to calculate the correction to the two-level geometric phase we split the Hamiltonian $\hat{H}(0)$ into a block diagonal part

$$\frac{1}{\hbar}\hat{H}_0 = \sum_n (n\delta + \alpha_n)|n\rangle\langle n| + \frac{1}{2}(\Omega|1\rangle\langle 0| + \text{h.c.}),$$

which preserves the coupling between the two lowest levels but keeps all the higher levels decoupled, and a perturbation[2]

$$\frac{1}{\hbar}\hat{V} = \frac{1}{2}\sum_{n\geq 1} (\Omega g_{n,n+1}|n+1\rangle\langle n| + \text{h.c.}),$$

[2]In this case the matrix elements of $\hat{V}$ and $\hat{H}_0$ are comparable in magnitude which could cast doubts on whether $\hat{V}$ can be treated as a perturbation. In fact, the relevant quantities which determine if perturbative treatment is justifiable are $\langle\Phi_i^{(0)}|\hat{V}|\Phi_j^{(0)}\rangle/(E_i^{(0)} - E_j^{(0)})$ (see definitions given below). These are indeed much smaller than 1 if $|\delta|, |\Omega| \ll \|\alpha_2|$, which we further assume to be true.

which includes the omitted couplings. This decomposition can be illustrated in matrix form as (the black dots represent non-zero matrix elements)

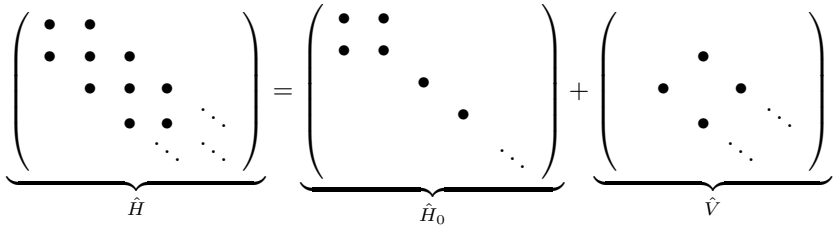

The eigenvectors of the unperturbed Hamiltonian $\hat{H}_0$ are

$$\begin{aligned} |\Phi_-^{(0)}\rangle &= \cos\frac{\theta}{2}|0\rangle - \sin\frac{\theta}{2}|1\rangle, \\ |\Phi_+^{(0)}\rangle &= \cos\frac{\theta}{2}|1\rangle + \sin\frac{\theta}{2}|0\rangle, \\ |\Phi_n^{(0)}\rangle &= |n\rangle \quad \text{for } n \geq 2 \end{aligned}$$

and the corresponding eigenvalues

$$\begin{aligned} E_-^{(0)} &= -\hbar\sqrt{\delta^2+\Omega^2}\sin^2\frac{\theta}{2}, \\ E_+^{(0)} &= \hbar\sqrt{\delta^2+\Omega^2}\cos^2\frac{\theta}{2}, \\ E_n^{(0)} &= \hbar(n\delta+\alpha_n) \quad \text{for } n \geq 2. \end{aligned}$$

We would like to calculate the geometric phase for a conical path

$$\gamma_n = 2\pi\langle\Phi_n|\hat{N}|\Phi_n\rangle$$

up to second order in $\hat{V}$. Substituting the perturbation series for $|\Phi_n\rangle$ gives us

$$\begin{aligned} \frac{1}{2\pi}\gamma_n &= \langle\Phi_n^{(0)}|\hat{N}|\Phi_n^{(0)}\rangle + 2\mathrm{Re}\,\langle\Phi_n^{(0)}|\hat{N}|\Phi_n^{(1)}\rangle + \\ &\quad \langle\Phi_n^{(1)}|\hat{N}|\Phi_n^{(1)}\rangle + 2\mathrm{Re}\,\langle\Phi_n^{(0)}|\hat{N}|\Phi_n^{(2)}\rangle + \mathcal{O}(\hat{V}^3). \end{aligned}$$

The first term on the right-hand side is just the two-level geometric phase from (3) with the sign $-$ for $n = -$ and $+$ for $n = +$. We will denote it by $\gamma_n^{(0)}$. For $n \geq 2$ equation (2) yields just a multiple of 2π so we can define $\gamma_n^{(0)}$ for such n to be zero.

The second term is equal to zero for the following reasons: For $n \geq 2$ it is simply proportional to $\mathrm{Re}\,\langle\Phi_n^{(0)}|\Phi_n^{(1)}\rangle$ which needs to be zero due to orthogonality of $|\Phi_n\rangle$. For $n = \pm$ the first order correction $|\Phi_n^{(1)}\rangle$ is proportional to $|\Phi_2^{(0)}\rangle$ (since $\hat{V}$ only couples $|\Phi_\pm^{(0)}\rangle$ to $|\Phi_2^{(0)}\rangle$) but the matrix elements $\langle\Phi_\pm^{(0)}|\hat{N}|\Phi_2^{(0)}\rangle$ are zero.

The first and second order corrections to the eigenvectors are

$$|\Phi_n^{(1)}\rangle = \sum_{m\neq n} \frac{V_{mn}}{E_{mn}} |\Phi_m^{(0)}\rangle, \tag{4.a}$$

$$|\Phi_n^{(2)}\rangle = \sum_{k,m\neq n} \frac{V_{km}V_{mn}}{E_{kn}E_{mn}} |\Phi_k^{(0)}\rangle - \sum_{k\neq n} \frac{V_{kn}V_{nn}}{E_{kn}^2} |\Phi_k^{(0)}\rangle - \frac{1}{2}\sum_{k\neq n} \frac{V_{nk}V_{kn}}{E_{kn}^2} |\Phi_n^{(0)}\rangle \tag{4.b}$$

where

$$\begin{aligned} V_{ij} &= \langle \Phi_i^{(0)} | \hat{V} | \Phi_j^{(0)} \rangle, \\ E_{ij} &= E_j^{(0)} - E_i^{(0)}. \end{aligned}$$

In our case the second term in equation (4.b) will not contribute because $V_{nn} = 0$ for all n.

We can then express our correction[3] to the geometric phase as

$$\begin{aligned} \frac{1}{2\pi}\Delta\gamma_n \equiv \frac{1}{2\pi}(\gamma_n - \gamma_n^{(0)}) &= \sum_{k,m\neq n} \frac{V_{nk}N_{km}V_{mn}}{E_{mn}E_{kn}} + 2\mathrm{Re} \sum_{k,m\neq n} \frac{N_{nk}V_{km}V_{mn}}{E_{kn}E_{mn}} \\ &\quad - \sum_{k\neq n} \frac{N_{nn}V_{nk}V_{kn}}{E_{kn}^2}. \end{aligned}$$

Here we have denoted the matrix elements of $\hat{N}$ by N_{ij} analogously to V_{ij}. Let us now choose $n = -$ or $n = +$ and denote the sign opposite to n by $\overline{n}$. Then since $\hat{V}$ only couples $|\Phi_\pm^{(0)}\rangle$ to $|\Phi_2^{(0)}\rangle$ our expression simplifies to

$$\frac{1}{2\pi}\Delta\gamma_n = \frac{V_{n2}(2 - N_{nn})V_{2n}}{E_{2n}^2} + 2\mathrm{Re}\,\frac{N_{n\overline{n}}V_{\overline{n}2}V_{2n}}{E_{\overline{n}n}E_{2n}}.$$

After substituting for V_{n2}, $V_{\overline{n}2}$, N_{nn} and $N_{\overline{n}n}$ we obtain

$$\begin{aligned} \frac{1}{2\pi}\Delta\gamma_- &= \frac{\hbar^2\Omega^2|g_{12}|^2}{4E_{2-}^2}\left(\sin^2\frac{\theta}{2} + \frac{2E_{2-} + E_{+-}}{E_{+-}}\sin^2\frac{\theta}{2}\cos^2\frac{\theta}{2}\right), \\ \frac{1}{2\pi}\Delta\gamma_+ &= \frac{\hbar^2\Omega^2|g_{12}|^2}{4E_{2+}^2}\left(\cos^2\frac{\theta}{2} + \frac{2E_{2+} + E_{-+}}{E_{-+}}\sin^2\frac{\theta}{2}\cos^2\frac{\theta}{2}\right), \end{aligned}$$

which can be further recast into the form

$$\frac{1}{2\pi}\Delta\gamma_- = \frac{k|g_{12}|^2\sin^2\theta}{4}\frac{2k(1-\cos\theta) + (2k + (3k+2)\cos\theta)\sin^2\theta}{(k + (3k+2)\cos\theta)^2}, \tag{5.a}$$

$$\frac{1}{2\pi}\Delta\gamma_+ = \frac{k|g_{12}|^2\sin^2\theta}{4}\frac{2k(1+\cos\theta) + (2k - (3k+2)\cos\theta)\sin^2\theta}{(k - (3k+2)\cos\theta)^2}, \tag{5.b}$$

[3]For the sake of brevity, we will further omit the $\mathcal{O}(\hat{V}^3)$-symbol from our expressions.

where $k = \delta/\alpha_2$ is the ratio between detuning and anharmonicity.

Expanding this result to first order in the parameter k gives us

$$\begin{aligned} \frac{1}{2\pi}\Delta\gamma_- &\approx \frac{\delta|g_{12}|^2}{8\alpha_2}\frac{\sin^4\theta}{\cos\theta}, \\ \frac{1}{2\pi}\Delta\gamma_+ &\approx -\frac{\delta|g_{12}|^2}{8\alpha_2}\frac{\sin^4\theta}{\cos\theta}, \end{aligned}$$

which agrees with the perturbative correction obtained by Stefano Pugnetti [7] using a different way of splitting the original Hamiltonian into $\hat{H}_0$ and $\hat{V}$. This alternative way is based on a rotation which diagonalizes the Hamiltonian in the two-level subspace $\mathcal{H}_2$. The transformed Hamiltonian is then split into a diagonal unperturbed part which is degenerate in $\mathcal{H}_2$ and the remaining perturbation which is traceless and off-diagonal outside of $\mathcal{H}_2$.

In both of these approaches, the off-diagonal elements of the perturbation in the eigenbasis of the unperturbed Hamiltonian are proportional to Ω whereas the eigenenergy differences are comparable in size with α_2 (if $|\delta| \ll |\alpha_2|$). Therefore in the limit $|\delta|, |\Omega| \ll |\alpha_2|$ both perturbations can be considered "small" and both perturbative results should approach the exact value in this limit. The two approaches are therefore in this sense equivalent.

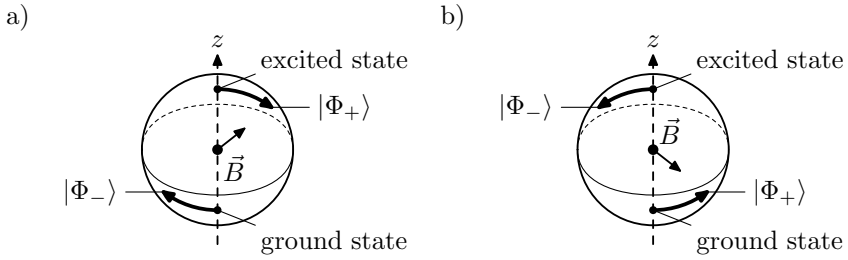

Figure 3: A Bloch sphere picture of the driven qubit eigenstates $|\Phi_-\rangle$ and $|\Phi_+\rangle$ and their adiabatic evolution from the ground and the excited state, respectively, for (a) positive detuning and vice versa for (b) negative detuning. The state $|\Phi_+\rangle$ is the one corresponding to the higher eigenvalue, i.e. its corresponding point on the Bloch sphere is given by the effective "magnetic field" $\vec{B}$ (whereas the point correspoding to the state $|\Phi_-\rangle$ is given by $-\vec{B}$). The sign of the detuning determines whether the initial vector $\vec{B}$ points towards the ground state (if $\delta < 0$) or the excited state (if $\delta > 0$) and therefore (since eigenenergies of a general smoothly evolving hamiltonian do not cross) which of these states adiabatically evolves into $|\Phi_+\rangle$.

As mentioned above, the quantity measured in the actual experiment was twice the difference between the geometric phases acquired by the ground and excited state of the qubit. If $\theta < \pi/2$ then $\delta > 0$ and as the qubit drive is adiabatically increased from zero to Ω, the ground (excited) state evolves into $|\Phi_-\rangle$ ($|\Phi_+\rangle$) and vice versa for $\theta > \pi/2$ (see Figure 3). Therefore

$$\Delta\phi \equiv 2(\Delta\gamma_g - \Delta\gamma_e) \approx \pm\frac{\pi\delta|g_{12}|^2}{\alpha_2}\frac{\sin^4\theta}{\cos\theta}, \tag{6}$$

where the sign + or − is chosen if $\theta < \pi/2$ or $\theta > \pi/2$. Equivalently, if we restrict the opening angle to the interval $[0, \pi/2]$ (i.e. replace θ by $\pi/2 - \theta$ if $\theta > \pi/2$) we can omit the sign $\pm$ in the previous equation.

We can see that the relative size of the geometric phase correction due to higher qubit levels is roughly of the order δ/α_2. This effect therefore becomes important if the detunings is comparable with the anharmonicity. The highest value of the ratio δ/α used in the experiment was approximately 1/6.

To reduce the correction due to higer qubit levels, one has to keep the qubit detuning δ much lower than α_2. However, in order to satisfy the adiabaticity condition, the total duration T of the adiabatic sequence has to be much longer than the typical Rabi period which is of the order $2\pi/\delta$. To maintain good coherence throughout the experiment, the total time T needs to be shorter than the coherence time τ of the qubit. Moreover, the anharmonicity of a transmon qubit is much lower than its $g - e$ transition frequency. In summary, we can write these conditions as

$$2\pi/\tau \ll 2\pi/T \ll |\delta| \ll |\alpha_2| \ll \omega_q.$$

This places constraints on the quantity $\omega_q\tau$ which needs to be relatively high (our is of the order 10^4 to 10^5) if geometric phase dependence close to that expected for an ideal two-level system is to be observed.

In other words, the quality of the qubit (quantified by the number of coherent oscillation cycles that the qubit can undergo before it loses coherence) has to be sufficiently high. It would be interesting to compare this constraint with constraints placed on the qubit quality by the circuit design, materials and manufacturing processes used in its making etc.

3.3 Comparison with numerical calculations and experimental results

To check the validity of our perturbative results, we performed a series of numerical calculations and simulations. First, we diagonalized the system's Hamiltonian (truncated at some finite number of qubit and resonator levels) numerically to calculate the geometric phases directly from equation (2). Furthermore, we directly simulated the qubit evolution during the experiment (except for the final state tomography) to make sure that other aspects of the measurement such as the spin echo sequence, non-adiabatic effects etc. do not play a significant role[4].

We tried to perform the simulations both by solving the Schrödinger equation (unitary dynamics) and the quantum master equation [8] taking into account qubit decay (non-unitary dynamics), only to find out that these phenomena have a negligible effect on the results. Describing the system by a pure state therefore seemed to be sufficient for our purposes.

Figure 4 shows a comparison of the corrections due to higher qubit levels as obtained using the perturbative result (5.a) and (5.b) with results of the numerical calculations

[4]More precisely – although non-adiabatic effects are observable in the simulations (especially for lower detunings), they do not seem to cause a systematic shift of the theoretically predicted value of the phase but only oscillations around this value.

mentioned above. For negative detunings (Fig. (c), (d)) the correction is positive while negative corrections are obtained for positive detunings (Fig. (a), (c)).

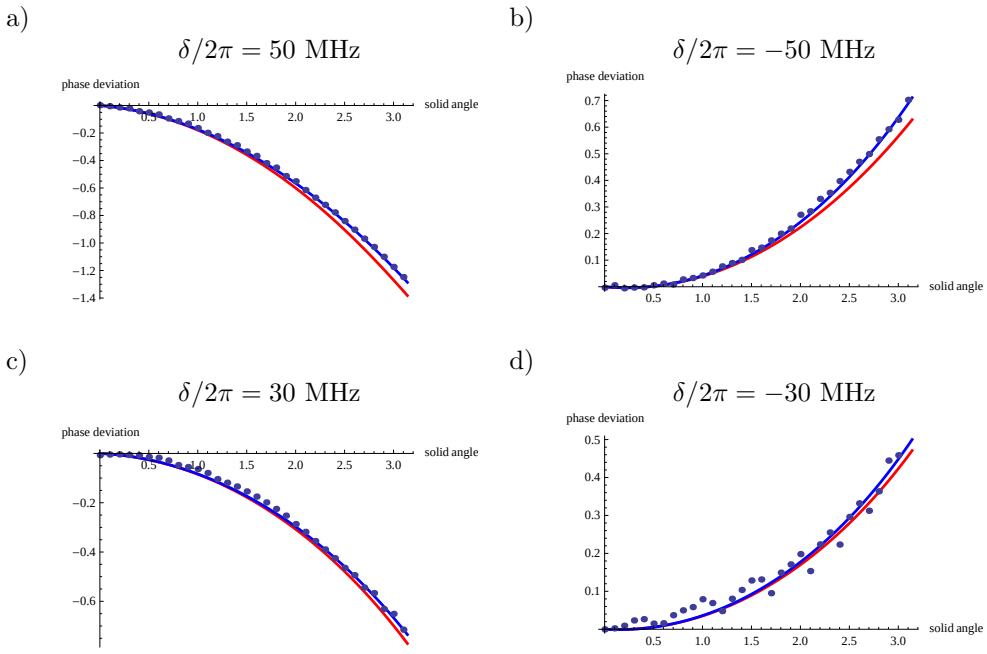

Figure 4: Corrections to the phase ϕ due to higher qubit levels: Comparison of the perturbative result in equations (5.a) and (5.b) (red line) with the results of numerical diagonalization of the Hamiltonian (blue line) and simulation of the qubit evolution during the experiment (blue points) for different values of the detuning δ. Calculations were performed for a three-level qubit with anharmonicity $\alpha_2/2\pi = -340$ MHz and an 800 ns long measurement sequence. Non-adiabatic effects are visible in (d).

We can see that simulations of the system's evolution produce results which are in good agreement with predictions of the general relation (2). We believe that the differences (prominent especially for detuning $\delta/2\pi = -30$ MHz) are caused by non-adiabatic effects. The perturbative correction due to higher qubit levels expressed in equations (5.a) and (5.b) also agrees quite well with both the simulation and numerical diagonalization results.

We have also compared the results obtained by numerical diagonalization for various numbers of qubit levels. This comparison showed that it is sufficient to consider a three-level qubit because the phase deviation calculated for higher numbers of levels differ from the three-level result by less than two percent (see Figure 5). Such difference cannot be resolved in our comparisons with experimental data which show other, more significant deviations.

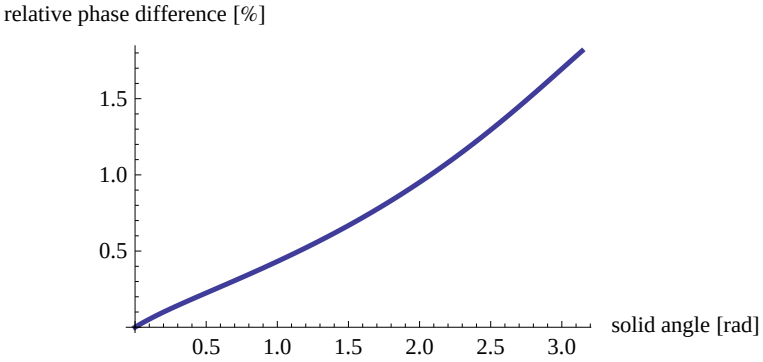

Figure 5: Relative difference between theoretical predictions for the deviation of the measured phase obtained by numerical diagonalization of the Hamiltonian with 3 and 10 qubit levels. The calculation was performed for detuning $\delta/2\pi = 50$ MHz.

When we compare the above theoretical predictions obtained by including effects of higher qubit levels with experimental data, we see a systematic discrepancy between those two. The predicted and measured deviation of the geometric phase from the simple two-level linear dependence seem to have the same sign but different magnitude.

Figure 6 shows two experimental data sets in comparison with the results predicted by theory.

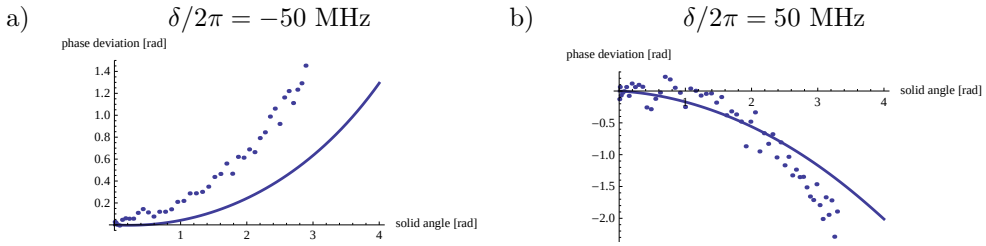

Figure 6: Comparison of the correction to the geometric phase due to higher qubit levels (solid line) with experimental results (points) for (a) positive and (b) negative detuning.

In our first attempt to explain this discrepancy, we considered the possibility that some yet unknown effect causes a shift in the two key parameters of the model – the anharmonicity α_2 and the relative coupling g_{12} between the second and the third level of the qubit – but otherwise leaves the functional dependence (5.a) and (5.b) of the measured phase on the solid angle unchanged.

However, as illustrated in Figure 7, comparison of experimental data obtained for different qubit detunings shows that no shift in α_2 and g_{12} can account for the differences between theory and experiment in all the data sets at the same time. Therefore, we need to modify our theory in some other way.

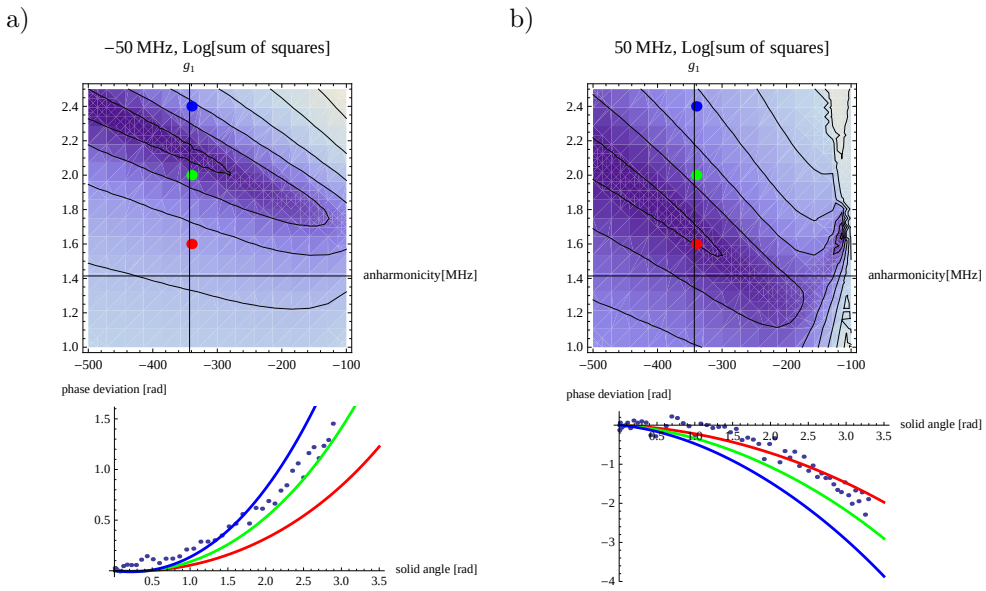

Figure 7: Density plots showing sums of squared deviations of the measured data from numerical diagonalization results as functions of the anharmonicity α_2 and the relative coupling g_{12} between the second and the third qubit level. The plots below show the calculated and the measured values explicitely for three arbitrarily chosen parameter values, marked in the density plots above by coloured points. Comparison of the results for (a) negative and (b) positive detuning suggests that this simple theoretical model does not agree with experimental data for a fixed value of the two parameters.

4 Corrections due to qubit-resonator interactions

After considering several possible explanations of this disagreement between our theory and the experiment, we started to study potential effects of interactions between the qubit and the microwave cavity on the geometric phase.

It turns out that there is an effect capable of producing deviations in the geometric phase of the same order of magnitude (for our parameters of the sample) as the correction due to higher qubit levels discussed above. This effect can be naively understood as a change of the effective opening angle caused by the cavity-induced AC Stark shift of the qubit. As the drive strength increases, the mean photon population of the off-resonantly driven resonator grows which in turn pushes the qubit frequency farther away from the resonator frequency. In our case the latter is higher which means that this effect tends to decrease the qubit-drive detuning. This translates to larger solid angles and therefore higher geometric phases if the detuning is positive and vice versa.

This unfortunately means that the effect of qubit-resonator interactions on the geometric phase is exactly opposite to what we would need to explain our experimental results. This is of course no reason to neglect this effect. In the next section we will

derive the resonator-induced correction to the geometric phase using perturbation theory in the dispersive limit. To this end, we will treat the qubit as a two-level system which will greatly simplify the calculations and allow us to see the effect of the cavity and its dependence on the parameters of the system separately from the higher qubit level contribution.

4.1 The dispersive cavity QED Hamiltonian

If the qubit and the resonator are far detuned from each other (i.e. the qubit and resonator frequencies ω_q, ω_r satisfy $|\omega_q - \omega_r| \gg g$ where g is the qubit-resonator coupling strength), the Jaynes-Cummings Hamiltonian [9] in the corotating frame

$$\hat{H} = \hbar\delta_r \hat{a}^\dagger \hat{a} + \frac{1}{2}\hbar\varepsilon(\hat{a} + \hat{a}^\dagger) + \frac{1}{2}\hbar\delta_q \hat{\sigma}_z + \hbar g(\hat{\sigma}_{eg}\hat{a} + \hat{a}^\dagger \hat{\sigma}_{ge})$$

(where δ_q and δ_r are again the detunings of the qubit and the resonator from the drive frequency, ε is the input signal driving the resonator and $\hat{\sigma}_{ij}$ for $i, j \in \{g, e\}$ denote operators $|i\rangle\langle j|$) can be unitarily transformed by $\hat{U}_{\text{disp}} = \exp(g(\hat{\sigma}_{eg}\hat{a} - \hat{a}^\dagger\hat{\sigma}_{ge})/(\omega_q - \omega_r))$ which effectively eliminates terms corresponding to energy exchange between the two subsystems.

Keeping only terms up to second order in g and neglecting higher levels of the qubit, the dispersive Hamiltonian has the form

$$\begin{aligned}\hat{H}_{\text{disp}} = \hat{U}_{\text{disp}}\hat{H}\hat{U}_{\text{disp}}^\dagger = \hbar\left(\delta_r + \frac{g^2}{\omega_r - \omega_q}\right)\hat{a}^\dagger\hat{a} + \frac{1}{2}\hbar\varepsilon(\hat{a} + \hat{a}^\dagger) + \\ \frac{1}{2}\hbar\left(\delta_q - \frac{g^2}{\omega_r - \omega_q}\right)\hat{\sigma}_z - \frac{1}{2}\frac{g}{\omega_r - \omega_q}\hbar\varepsilon\hat{\sigma}_x - \\ \frac{2\hbar g^2}{\omega_r - \omega_q}\hat{a}^\dagger\hat{a}\hat{\sigma}_{ee} + \frac{1}{4}\hbar\varepsilon\left(\frac{g}{\omega_r - \omega_q}\right)^2(\hat{a} + \hat{a}^\dagger)\hat{\sigma}_z.\end{aligned} \tag{7}$$

Here the first two lines represent the Hamiltonian of effectively decoupled resonator and qubit. Note that they already include the Lamb shift and the dispersive shift of the resonator frequency. The renormalized detunings

$$\begin{aligned}\delta_q^r &= \delta_q - \frac{g^2}{\omega_r - \omega_q}, \\ \delta_r^r &= \delta_r + \frac{g^2}{\omega_r - \omega_q}\end{aligned}$$

are therefore quantities that are actually measured in an experiment as opposed to the bare detunings δ_r and δ_q which are not directly accessible to a measurement (the same holds for frequencies ω_r and ω_q).

The third line includes ac Stark shifts [10] which appear whenever one of the subsystems is in an excited state. Furthermore, it includes a qubit-dependent correction of the coupling between the resonator and the external drive (this term is usually not included in the dispersive Hamiltonian but it turns out that in our case it needs to be considered as well).

4.2 Perturbative calculation of the resonator-induced correction

The qubit-resonator Hamiltonian (7) has again a form which allows us to extract the dependence on the drive phase φ by means of a rotation $\exp(-\mathrm{i}\varphi\hat{N})$ where this time

$$\hat{N} = \hat{a}^\dagger\hat{a} + \sum_n n|n\rangle_q\langle n|_q.$$

The geometric phases of its eigenstates are then again given by the expectation values of this operator multiplied by 2π, cf. equation (2).

The first two lines in equation (7) (let us denote them by $\hat{H}_0$) can be exactly diagonalized (up to an overall energy shift) by rotating the qubit state around the y-axis and displacing the resonator state by the unitary operation $\hat{U}_R = \exp(\varepsilon(\hat{a}^\dagger - \hat{a})/2\delta_r^r + \mathrm{i}\theta\hat{\sigma}_y/2)$:

$$\hat{U}_R\hat{H}_0\hat{U}_R^\dagger = \hbar\delta_r^r\hat{a}^\dagger\hat{a} + \frac{1}{2}\hbar\Delta_q^r\hat{\sigma}_z,$$

where δ_q^r is determined by $\delta_q^r = \Delta_q^r\cos\theta$ and $-\frac{g}{\omega_r-\omega_q}\varepsilon = \Delta_q^r\sin\theta$.

The eigenstates of $\hat{H}_0$ and their corresponding eigenenergies are therefore

$$|n,s\rangle \equiv \hat{U}_R^\dagger|n\rangle\otimes|s\rangle = \exp\left(\frac{\varepsilon}{2\delta_r^r}(\hat{a}-\hat{a}^\dagger)\right)|n\rangle\otimes\exp\left(-\frac{\mathrm{i}}{2}\theta\hat{\sigma}_y\right)|s\rangle,$$

$$E_{n,s} = \hbar\delta_r^r n \pm \frac{1}{2}\hbar\Delta_q^r,$$

where $n\in\{0,1,\ldots\}$, $s\in\{g,e\}$ and the signs $+$ and $-$ in the expression for the energy correspond to $s=e$ and $s=g$ respectively.

The expectation value of $\hat{N}$ in first order of the perturbation

$$\hat{V} = -\frac{2\hbar g^2}{\omega_r-\omega_q}\hat{a}^\dagger\hat{a}\hat{\sigma}_{ee} + \frac{1}{4}\hbar\varepsilon\left(\frac{g}{\omega_r-\omega_q}\right)^2(\hat{a}+\hat{a}^\dagger)\hat{\sigma}_z$$

is given by

$$\langle\hat{N}\rangle_{n,s} = \langle n,s|\hat{N}|n,s\rangle + 2\,\mathrm{Re}\sum_{(n',s')\neq(n,s)}\frac{\langle n,s|\hat{N}|n',s'\rangle\langle n',s'|\hat{V}|n,s\rangle}{E_{n,s}-E_{n',s'}}.$$

The matrix element of $\hat{N}$ is only non-zero if $n'=n$ or $s'=s$. Therefore

$$\begin{aligned}
\langle\hat{N}\rangle_{n,s} &= \langle n,s|\hat{N}|n,s\rangle + 2\,\mathrm{Re}\sum_{n'\neq n}\frac{\langle n,s|\hat{N}|n',s\rangle\langle n',s|\hat{V}|n,s\rangle}{\hbar\delta_r^r(n-n')} + 2\,\mathrm{Re}\,\frac{\langle n,s|\hat{N}|n,s'\rangle\langle n,s'|\hat{V}|n,s\rangle}{\pm\hbar\Delta_q^r} \\
&= n + \left(\frac{\varepsilon}{2\delta_r^r}\right)^2 + \frac{1\pm\cos\theta}{2} - \frac{\varepsilon}{\delta_r^r}\,\mathrm{Re}\sum_{n'\neq n}\frac{\langle n|(\hat{a}+\hat{a}^\dagger)|n'\rangle\langle n',s|\hat{V}|n,s\rangle}{\hbar\delta_r^r(n-n')} \mp \mathrm{Re}\,\frac{\langle n,s'|\hat{V}|n,s\rangle}{\hbar\Delta_q^r}\sin\theta \\
&= n + \left(\frac{\varepsilon}{2\delta_r^r}\right)^2 + \frac{1\pm\cos\theta}{2} - \frac{\varepsilon}{\hbar(\delta_r^r)^2}\,\mathrm{Re}\left(\sqrt{n}\langle n-1,s|\hat{V}|n,s\rangle - \sqrt{n+1}\langle n+1,s|\hat{V}|n,s\rangle\right) \\
&\quad \mp \mathrm{Re}\,\frac{\langle n,s'|\hat{V}|n,s\rangle}{\hbar\Delta_q^r}\sin\theta \\
&= n + \left(\frac{\varepsilon}{2\delta_r^r}\right)^2 + \frac{1\pm\cos\theta}{2} + \frac{\varepsilon^2 g^2}{(\delta_r^r)^3(\omega_r-\omega_q)}\left(\frac{1\pm\cos\theta}{2} \pm \frac{1}{4}\frac{\delta_r^r}{\omega_r-\omega_q}\cos\theta\right) \\
&\quad \mp \frac{g^2}{\Delta_q^r(\delta_r^r)^2(\omega_r-\omega_q)}\sin^2\theta\left(n(\delta_r^r)^2 + \frac{1}{4}\varepsilon^2\left(1+\frac{\delta_r^r}{\omega_r-\omega_q}\right)\right).
\end{aligned}$$

From here we obtain the following expression for the geometric phase difference $\gamma_{|n,g\rangle} - \gamma_{|n,e\rangle}$

$$\frac{\gamma_{|n,g\rangle} - \gamma_{|n,e\rangle}}{2\pi} = -\cos\theta - \frac{\varepsilon^2 g^2}{(\delta_r^r)^3(\omega_r - \omega_q)}\cos\theta\left(1 + \frac{1}{2}\frac{\delta_r^r}{\omega_r - \omega_q}\right) + \frac{1}{\Delta_q^r(\delta_r^r)^2(\omega_r - \omega_q)}\sin^2\theta\left(2ng^2(\delta_r^r)^2 + \frac{1}{2}\varepsilon^2 g^2\left(1 + \frac{\delta_r^r}{\omega_r - \omega_q}\right)\right)$$

Considering that $\varepsilon g = -(\omega_r - \omega_q)\delta_q^r \tan\theta$ and $\Delta_q^r = \delta_q^r/\cos\theta$, we get for $n = 0$

$$\frac{\Delta\gamma_{|0,g\rangle} - \Delta\gamma_{|0,e\rangle}}{2\pi} = \frac{(\omega_r - \omega_q)\delta_q^r}{(\delta_r^r)^2}\frac{\sin^2\theta}{\cos\theta}\left[\frac{1}{2}\sin^2\theta\left(1 + \frac{\delta_r^r}{\omega_r - \omega_q}\right) - \frac{\delta_q^r}{\delta_r^r}\left(1 + \frac{1}{2}\frac{\delta_r^r}{\omega_r - \omega_q}\right)\right]. \quad (8)$$

4.3 Comparison with numerical calculations

Once again, we performed simulations aimed at checking the validity of the perturbative result (8) for the resonator induced correction to the measured phase. This time the model included only two qubit levels and the system was described by the full Jaynes-Cummings Hamiltonian. The results of this simulation are shown in Figure 8.

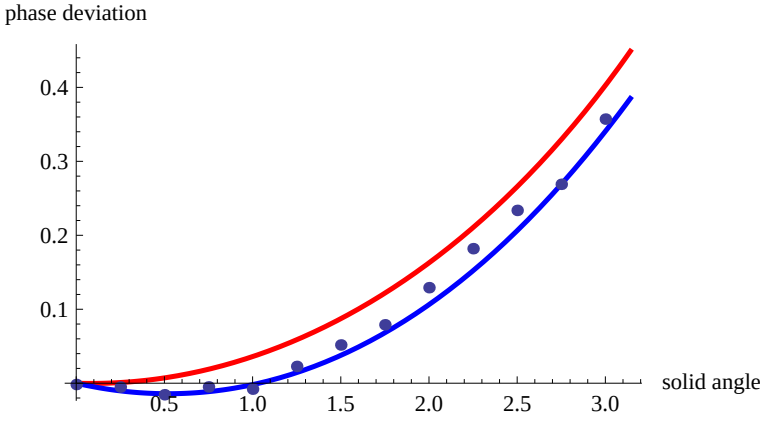

Figure 8: Corrections to the geometric phase due to qubit-resonator interactions for a two-level qubit: Comparison of the perturbative result in equation (8) (red line) with the results of numerical diagonalization of the Hamiltonian (blue line) and simulation of the qubit-resonator evolution during the experiment (blue points) for detuning $\delta/2\pi = 50$ MHz. The simulation was performed for four resonator levels and a 600 ns long measurement sequence.

Apparently, in this case the agreement between theory and experiment is not as good as for the previously discussed higher qubit level correction. However, the perturbative

result is still useful in that it can provide a good insight into how different parameters of the system influence the resonator-induced correction.

To determine whether using four resonator levels in our simulations is sufficient, we compared the results obtained for 4 and 10 levels and found that they differed by less than four percent (see Figure 9). This indicates that unless we are interested in opening angles closer to $\pi/2$ or detunings significantly higher than 50 MHz, describing the resonant cavity by a four-level system should indeed be sufficient.

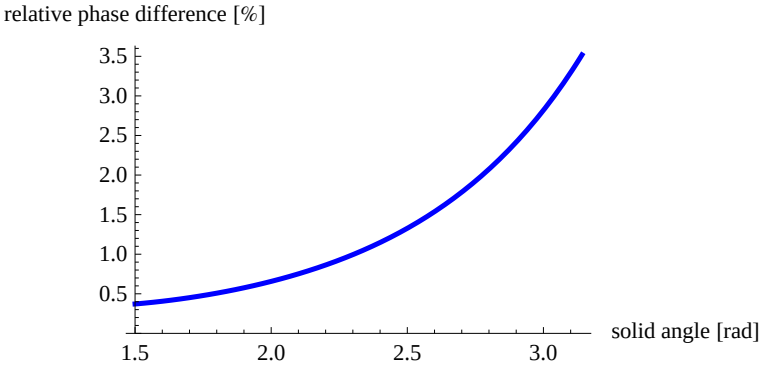

Figure 9: Relative difference between theoretical predictions for the deviation of the measured phase obtained by numerical diagonalization of the Jaynes-Cummings Hamiltonian with 4 and 10 resonator levels (and a two-level qubit). The calculation was performed for detuning $\delta/2\pi = 50$ MHz.

Finally, we considered a model including higher qubit levels as well as qubit-resonator interactions. We performed the same simulations as in the previous cases and compared them with results obtained by simply summing the two types of corrections in equations (5.a), (5.b) and (8). The comparison is presented in Figure 10.

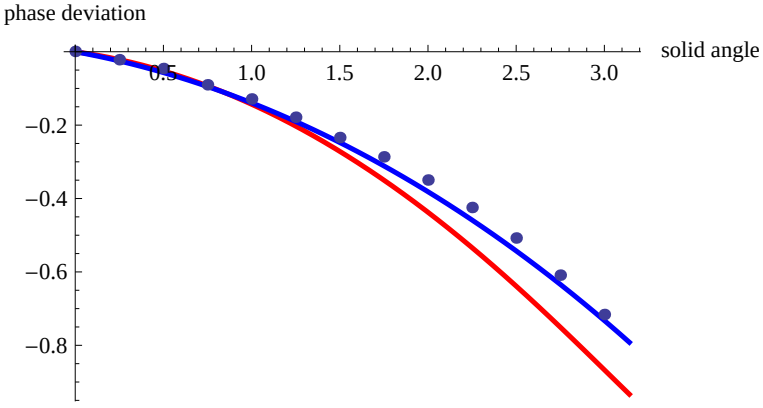

Figure 10: Corrections to the geometric phase due to higher qubit levels and qubit-resonator interactions: Comparison of the sum of the perturbative results (5.a,5.b) and (8) (red line) with the results of numerical diagonalization of the Hamiltonian (blue line) and simulation of the qubit-resonator evolution

during the experiment (blue points) for detuning $\delta/2\pi = 50$ MHz. The simulation was performed for 3 qubit levels, 4 resonator levels and a 600 ns long measurement sequence.

This comparison suggests that lowest order perturbation theory can only be used to describe both effects – due to higher qubit levels and qubit-resonator interactions – with relatively limited precision. For this reason, we decided to use numerical calculations instead of our perturbative results for further comparisons between theory and experiment.

5 Numerical calculations and their comparison with experimental results

We have performed numerical calculations of the geometric phase for each of the experimental data sets to compare with. But as the perturbative results already indicated, the correction due to higher qubit levels is too small and the resonator-induced correction even has the wrong sign. The resulting agreement is not very good (see Figure 11).

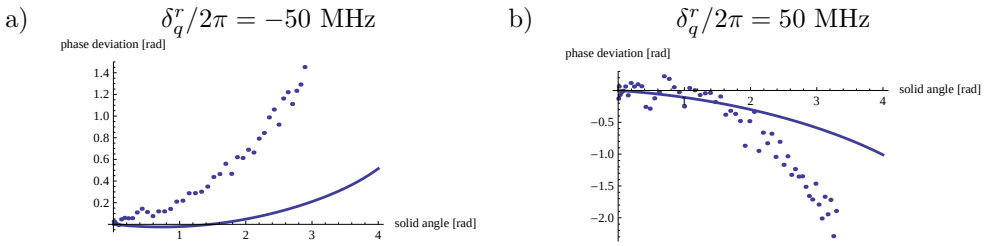

Figure 11: Comparison of two experimental data sets with numerical calculations taking into account higher qubit levels and interaction between the qubit and the resonator.

We then started to consider possible explanations for this discrepancy. It seems that there might be some unwanted interactions which are not included in the model of a multilevel qubit coupled to one resonator mode. For example, other modes of the resonator could also play a role. Or the qubit might not be an ideal anharmonic oscillator but could have some additional degrees of freedom.

In general, the presence of a transition with a frequency lower than the qubit frequency would cause a shift of the geometric phase in the "correct" direction (by the Stark shift mechanism described above).

The simplest way in which we can extend our model is to add another 2-level system (fluctuator) coupled to the qubit. We tried to estimate how the geometric phase is altered by the presence of such 2-level system. The results of the calculations show (see Figure 12) that its effect can be quite pronounced if the frequencies of the qubit and the fluctuator are close to each other but since we consider the fluctuator coupling to be relatively weak, its influence becomes much smaller when the qubit and the fluctuator are far detuned from each other.

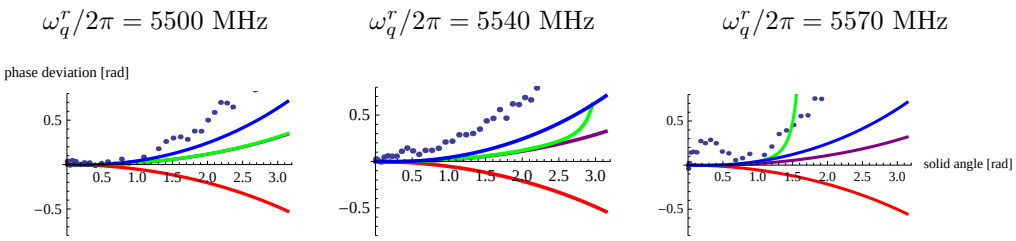

Figure 12: Results of numerical calculations of the geometric phase deviation from the linear dependence for a 3-level qubit (blue line), a 2-level qubit coupled to a resonator with frequency $\omega_r^r/2\pi = 6950$ MHz and coupling strength $g/2\pi = 115$ MHz (red line), a 3-level qubit coupled to a resonator (violet line) and a 3-level qubit coupled to a resonator and another 2-level system (fluctuator) with frequency $\omega_f^r/2\pi = 5690$ MHz and coupling strength $g_f/2\pi = 5$ MHz (green line). These parameters of the fluctuator are indicated by a spectroscopy measurement which shows an avoided crossing of unclear origin at approximately 5.69 GHz. The calculations are performed for three different qubit frequencies ω_q^r and for detuning $\delta_q^r/2\pi = -50$ MHz. The corresponding experimental data points are included for comparison.

With increasing drive strength, the frequency of the qubit is getting closer to the frequency of the fluctuator. The presence of the avoided crossing modifies (in our case increases) the geometric phase.

However, this finding also points to an unpleasant feature of our numerical calculations based on diagonalization of the Hamiltonian. This approach obviously yields results valid for the *ideally adiabatic* case when the Hamiltonian is being changed slowly enough so that the eigenstates can follow all the avoided crossings. But as is the case for our potential 2-level fluctuator, the coupling strengths of any additional systems coupling to the qubit are expected to be relatively small. In reality, the experimental sequence is probably not slow enough to maintain adiabaticity at *all* avoided crossings. The numerical calculation then shows an abrupt change in the geometric phase whenever such "experimentally invisible" close avoided crossing occurs (see Figure 13).

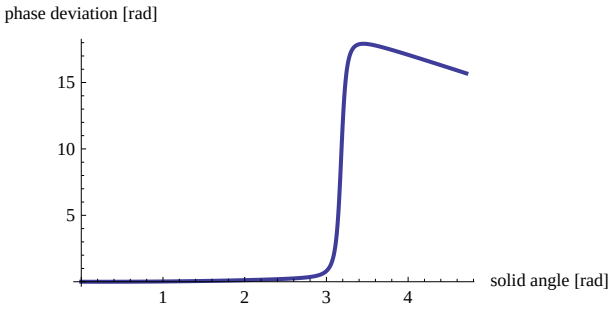

Figure 13: Result of a numerical calculation of the geometric phase deviation for a 3-level qubit with frequency $\omega_q^r/2\pi = 5540$ MHz coupled to a resonator and a 2-level system with frequency $\omega_f^r/2\pi = 5690$ MHz. The detuning was $\delta_q^r/2\pi = -50$ MHz. The abrupt change in the geometric phase is caused by an avoided crossing between energy levels of the qubit and the fluctuator.

6 Conclusions

We studied how the geometric phase in a superconducting transmon qubit coupled to a resonant cavity differs from that of an ideal two-level system [2]. We derived a simple expression for the geometric phase accumulated by a system following a conical path (2) and used it to calculate corrections due to higher qubit levels and due to qubit-resonator interactions to lowest order in perturbation theory. We found that these corrections are roughly proportional to the ratios δ_q/α (qubit detuning to anharmonicity) and δ_q/δ_r (qubit detuning to resonator detuning), respectively.

We also tried to use numerical calculations of the discussed effects to explain the deviation of the experimentally measured geometric phases from the ideal two-level values. So far, we have not been able to produce a satisfactory quantitative match between the theoretical predictions and experimental data. Some measurements of the qubit relaxation time and the transmission spectrum of the resonator suggest that there might be some unwanted additional degrees of freedom whose coupling to the qubit obscures the results.

Whether this is true or not might become clearer after more measurements are made with a new simpler sample.

References

[1] A. Messiah. *Quantum Mechanics, Vol. II.* North Holland Publishing Company, Amsterdam, 1962.

[2] M. V. Berry. Quantal phase factors accompanying adiabatic changes. *Proc. R. Soc. Lond. A*, 392:45, 1984.

[3] S. Filipp et al. Experimental demonstration of the stability of Berry's phase for a spin-1/2 particle. *Phys. Rev. Lett.*, 102:030404, 2009.

[4] J. Koch et al. Charge insensitive qubit design derived from the Cooper pair box. *Phys. Rev. A*, 76:042319, 2007.

[5] A. Blais et al. Cavity quantum electrodynamics for superconducting electrical circuits: An architecture for quantum computation. *Phys. Rev. A*, 69:062320, 2004.

[6] P. J. Leek et al. Observation of Berry's phase in a solid state qubit. *Science*, 318:1889, 2007.

[7] S. Pugnetti. Notes. 2010.

[8] H.-P. Breuer and F. Petruccione. *The Theory of Open Quantum Systems.* Oxford University Press, 2002.

[9] A. Blais et al. Quantum information processing with circuit quantum electrodynamics. *Phys. Rev. A*, 75:032329, 2007.

[10] D. I. Schuster et al. AC-stark shift and dephasing of a superconducting qubit strongly coupled to a cavity field. *Phys. Rev. Lett.*, 94:123602, 2005.